Reactions of CH₂OO, CH₃CHOO, and (CH₃)₂COO with Methane through the Formation of Intermediate Complex

Yuri A. Dyakov [1,2], **Sergey O. Adamson** [1], **Gennady V. Golubkov** [1], **Igor I. Morozov** [1], **Danil R. Nigmatullin** [1], **Oleg A. Olkhov** [1], **Pao K. Wang** [2,3,4] and **Maxim G. Golubkov** [1,*]

1   Semenov Federal Research Center for Chemical Physics, Russian Academy of Sciences, 119334 Moscow, Russia; yuri_dyakov@mail.ru (Y.A.D.); sergey.o.adamson@gmail.com (S.O.A.); kolupanovo@gmail.com (G.V.G.); igormrzv@gmail.com (I.I.M.); dan-nigm@mail.ru (D.R.N.); oleg.olkhov@rambler.ru (O.A.O.)
2   Research Center for Environmental Changes, Academia Sinica, Taipei 115, Taiwan; pkwang@gate.sinica.edu.tw
3   Department of Atmospheric Science, National Taiwan University, Taipei 10617, Taiwan
4   Department of Atmospheric and Oceanic Sciences, University of Wisconsin-Madison, Madison, WI 53706, USA
*   Correspondence: maxgol2008@mail.ru; Tel.: +7-495-9397322

Abstract: Criegee intermediates, which are the products of the ozonolysis of alkenes, play a key role in many chemical and physical processes in the atmosphere. Their reactions with other atmospheric compounds are responsible for the formation of hydroxyl, methyl, hydrogen radicals, nitric and sulfuric acids, and others. Methane is an active greenhouse gas whose concentration has increased rapidly in the last several decades. In this work, we consider the interaction between these two important atmospheric compounds. We choose the three simple Criegee intermediate (CI) molecules: formaldehyde oxide (CH_2OO), acetaldehyde oxide (CH_3CHOO), and acetone oxide (($CH_3)_2COO$). Some reactions between methane and these Cis have been studied earlier as possible pathways for deactivating methane as well as a source of methanol formation due to molecular collisions in the atmosphere. In the present study, we extend the consideration to the case when an intermediate energetically stable complex is formed after collision. We found that this complex could easily decompose to form an OH radical and another unstable fragment, which can quickly dissociate into CH_3 radicals, atomic hydrogen, acetone, acetaldehyde, propaldehyde, methyl alcohol, water, and others, depending on the type of CI being reacted with. These compounds can actively interact with other atmospheric components and change their physical and chemical properties. In addition, CI with a methyl substituent is shown to have increased energy in transition states and minima, resulting in slower reaction rates.

Keywords: Criegee intermediate; collisional dissociation; CH_2OO; CH_3CHOO; ($CH_3)_2COO$; methane; OH and CH_3 radicals; acetone; formaldehyde; acetaldehyde; isomerization; dissociation

1. Introduction

Methane (CH_4), along with many other volatile components of the Earth's atmosphere (carbon dioxide (CO_2), water vapor, ozone (O_3), nitrous oxide (N_2O), etc.), is a potent greenhouse gas that traps part of the infrared terrestrial radiation and contributes to global warming. The greenhouse potential of methane is extremely high and far exceeds that of carbon dioxide [1]. At the same time, reports from the World Meteorological Organization (WMO) indicate that CH_4 concentration in the atmosphere has already significantly surpassed preindustrial levels. Thus, methane can have a great impact on atmospheric chemistry and the climate of the Earth.

CH_4 emissions into the atmosphere can be from either anthropogenic activity such as agriculture, biogas release at waste disposal sites, coal mining, etc., or natural sources.

Among the important natural sources are permafrost and gas hydrates on the seabed, both of which are being destroyed by releasing their methane into the atmosphere due to global warming. The impact of methane and other greenhouse gases on the Earth's climate is not limited to the troposphere but also the stratosphere, mesosphere, and even ionosphere due to the upward transport of these gases. This means that the mechanisms of mixing volatile atmosphere compounds between these layers and chemical interactions occurring in the lower and upper atmospheres are of great scientific importance.

Methane can penetrate into the stratosphere via turbulent diffusion from the troposphere to the stratosphere and sequentially to the mesosphere and ionosphere during tropical hurricanes, thunderstorms, and volcanic eruptions [2,3]. This transport process can be significantly enhanced by the propagation of internal and acoustic gravity waves (IGWs and AGWs) [4–6]. In the polar latitudes, troposphere gases can also be transported to the upper atmospheric layers through the polar vortex [7]. Since the polar region is also the largest reservoir of methane, this polar vortex transport is believed to have significantly contributed to the increase in methane concentration in the stratosphere in the last few decades.

We shall now describe another key class of atmospheric pollutants, namely volatile organic compounds (VOCs). These are the various unsaturated molecules, such as alkenes and polyaromatic unsaturated hydrocarbons (PAHs). They are abundantly emitted into the troposphere from biogenic and anthropogenic sources. Terrestrial vegetation is the dominant source of atmospheric VOCs (up to 90% of total emissions, depending on regions) [8,9]. VOCs are also abundantly produced by the combustion of organic fuel in internal combustion engines and by the operation of chemical and other heavy industries. Isoprene is the most prominent non-methane volatile unsaturated hydrocarbon and is a significant source of formaldehyde oxide, one of the CIs under consideration. PAHs are the main components of soot particles. Once formed in the lower atmosphere, they can be transported into the upper atmosphere layers through the same mechanisms described above for methane. Their major degradation pathways are reactions initiated with OH, O_3, NO_3, and halogens [10,11].

CIs form during the ozonolysis of alkenes, and their role in the atmosphere was first studied by Rudolf Criegee in the early 1950s [12]. Because of their extremely high instability [13,14], it is only recently that CIs have been studied by direct experimental methods. Their high chemical activity is due to the presence of the biradical >C-O-O group, which readily interacts with various substances present in the atmosphere, such as water [13,15–18] and many other chemical compounds [19–25]. Their reactions with SO_2 and NO_2 molecules produce sulfuric and nitric acids [26–28].

The formation of CIs results in a significant energy release of about 40–50 kcal/mol [29]. Some of this energy can be converted into the internal vibrational energy of the molecule, causing its further decomposition with the formation of methane, atomic oxygen, OH, vinoxy (CH_2CHO), CH_3, and HCO radicals, CO, CO_2, H_2, acetic acid (CH_3COOH), and other fragments [30–37]. In dense atmospheric layers, i.e., the troposphere and lower stratosphere, this energy could quickly dissipate through collisions, and, as a result, the CI molecules would become thermodynamically stable and then react with water or other atmospheric compounds. On the other hand, if the available internal energy remains high enough, they can decompose to form OH radicals and other fragments. Part of the energy obtained during the synthesis of CIs might also be converted into the vibrational, translational, and rotational energy of other fragments that arise as a result of the reaction.

In the upper stratosphere and mesosphere, however, the air density is very low and the concentration of molecules is rather small; intermolecular collisions are rare, and therefore CI molecules could retain a significant part of the internal energy obtained during the formation. Moreover, many molecules in the upper atmosphere can be electronically excited or ionized by the absorption of ultraviolet (UV) photons, which are present abundantly at high altitudes, and this certainly applies to CI and methane molecules. The electronic spectroscopy and photochemistry of simple CIs like formaldehyde oxide, acetaldehyde

oxide, and acetone oxide have been studied in the last two decades in detail by several research groups [38–45]. It was found that these CIs have strong transitions in the UV wavelength range of 300–400 nm, with a maximum at 320–340 nm depending on the specific molecule. The appropriate absorption cross section for most of the studied CIs exceeds the value of 10^{-17} cm^2 molecule^{-1}). Electronic excitations by UV photons are usually accompanied by a nonadiabatic transition to the underlying electronic state. The transition occurs through the conical intersection of electronic terms with simultaneous excitation of intramolecular vibrations, as described in detail in [46–48]. Ions could also be recombined into highly excited neutral atoms and molecules through recombination with slow electrons [49]. The internal vibrational energy of these molecules can then be transferred into their kinetic energy through intermolecular collisions [50].

The reactions of CIs with other air compounds in the stratosphere and mesosphere produce a great variety of secondary products, such as acetaldehyde, formaldehyde, vinyl alcohol, acetone, acetic acid, etc. [25,51,52]. They are likely to contribute to the formation of high-altitude clouds.

In this work, we investigate the chemical interaction between CIs and methane induced by their collision. We choose three simple CI molecules, i.e., formaldehyde oxide CH$_2$OO, acetaldehyde oxide CH$_3$CHOO, and acetone oxide (CH$_3$)$_2$COO. They differ from each other in the replacement of hydrogen atoms with one or two methyl groups. The properties of some of these molecules have been studied earlier [53–55]. It was found [53] that the interaction of CH$_2$OO molecules with various greenhouse gases leads to the formation of the van der Waals complex, which, in the case of methane, is likely to be unstable. The collision of CH$_2$OO with methane at medium kinetic energy initiates the reaction that produces methanol [54]. This reaction was found to be energetically more preferable than the formation of a stable molecular complex. But the probability of collisional reactions depends strongly on the initial mutual orientation of molecules. In order to assess the chance of reactions occurring more reliably, molecular dynamics or other dynamics simulation methods are required. And even in that case, the reaction probability will depend on the total kinetic energy of the colliding molecules.

In the last decade, processes related to the excited states of CIs have attracted great interest. A series of works dedicated to highly excited electronic states of CIs, especially the transitions between different electronic states through conical intersections and even the transitions to triplet states, were published recently [56–58]. These reactions are also of great interest to the study of photochemical and physical processes in the upper atmosphere and ionosphere. However, in our present work, we consider methane and Cis in the ground state as the initial reagents of the reaction. Nevertheless, the possibility of electronic excitation of the intermediate complex was taken into account. In view of the potential future importance of excited states, we carried out calculations of the reaction product yields in the 100–250 kcal/mol energy range.

The case of the direct formation of methanol during collisions of CI and methane has been described in [54] and hence will not be considered here. In our figures, we also omit several small van der Waals minima, which arise during the process of bringing molecules together [53,54]. These minima are small (less than 2.5 kcal/mol), their depth depends on the relative orientation of the molecules, and, due to their shallow depth, do not affect the kinetics of the reactions that we are considering. In this work, we shall study in detail the mechanism of chemical reactions between Cis and methane through the formation of stable intermediate complexes. We will extend previous investigations by studying three similar CIs, which differ from each other by the number of substituting methyl groups. Finally, we will draw some conclusions about the methylation effect on the chemical activity of the simplest CI.

2. Calculation Method

The geometries of all intermediates, transition states, initial reactants, and reaction products were optimized using the density functional B3LYP method [59–62] with the

aug-cc-pVTZ basis set. The intrinsic reaction coordinate (IRC) calculations have been performed to confirm the connection between transition states and the corresponding local minima. Energies of intermediates, transition states, reagents, and products at B3LYP/aug-cc-pVTZ optimized geometries were calculated using the ab initio UCCSD(T)/aug-cc-pVTZ method. Zero-point energy (ZPE) corrections using B3LYP/aug-cc-pVTZ frequencies were applied for the correction of the UCCSD(T) energy. All calculations were performed using the GAUSSIAN 09 package [63]. RRKM and microcanonical variational transition state theories [64–66] have been applied to compute the rate constants for individual reaction steps. UCCSD(T)/aug-cc-pVTZ energies and B3LYP/aug-cc-pVTZ frequencies have been used to perform the RRKM calculations. Relative product yields (branching ratios) were determined using the steady-state approach. The OH-elimination reaction occurs without distinct transition states. In this case, variational transition state theory (VTST) [66] was applied. To perform VTST calculations, UCCSD(T)/aug-cc-pVTZ energies calculated at the B3LYP/aug-cc-pVTZ optimized geometries were used. Additional computational details of this ab initio/RRKM/VTST approach have been described earlier [67].

3. Results and Discussion

3.1. $CH_2OO + CH_4$ Reaction

The potential energy surface (PES) along possible reaction pathways of the chemical reaction between CH_2OO Criegee intermediate and methane is presented in Figure 1. As mentioned above, we will not discuss the direct transformation of the reagents to methanol and formaldehyde. Instead, we shall concentrate on the second possible reaction path: through the formation of the relatively stable complex CH_3CH_2OOH (designated as **1**). In order to create this complex, the reagents need to cross the barrier **TS1** with an energy of 26.6 kcal/mol, which is rather high. However, as mentioned above, the synthesis of CIs provides a high release of energy. Part of this energy can be transformed into the kinetic energy of fragments. We also note that these reactions occur in the upper atmosphere, where the environment is not in thermodynamic equilibrium. Under the intense irradiation of UV photons as well as the recombination of positively charged molecular ions with electrons, electronic excitation of molecules leads to the accumulation of a large amount of energy, which can then transform into vibrational energy [46–48]. If this energy is below the dissociation limit of the molecule, then it can transform into kinetic energy due to collisions with other molecules in the medium [50].

After crossing the barrier TS1, a relatively deep minimum with an energy of −44.6 kcal/mol appears. Due to the negligible probability of a backward reaction from complex **1** to the initial reagents via **TS1** throughout the entire energy range of interest (see Figure 2 and discussion below), we assume for simplicity here and for the other two CI molecules that the reaction starts from isomer **1**, and the backward reaction through **TS1** is one of the possible reaction pathways.

Table 1. RRKM and VTST unimolecular rate constants (s^{-1}) and reaction path degeneracies of dissociation initiated by collision of CH_2OO and methane. Energy values are measured from the energy of isomer 1 (CH_3CH_2OOH).

| Transition State	Reaction	Reaction Path Degeneracy	Internal Energies, kcal/mol						
			100	125	150	175	200	225	250
TS1	$1 \rightarrow 2$	1	$1.1 \cdot 10^6$	$6.0 \cdot 10^7$	$6.6 \cdot 10^8$	$3.4 \cdot 10^9$	$1.1 \cdot 10^{10}$	$2.9 \cdot 10^{10}$	$6.1 \cdot 10^{10}$
TS2	$1 \rightarrow 3$	2	$7.6 \cdot 10^9$	$5.2 \cdot 10^{10}$	$2.0 \cdot 10^{11}$	$4.7 \cdot 10^{11}$	$9.7 \cdot 10^{11}$	$1.6 \cdot 10^{12}$	$2.6 \cdot 10^{12}$
TS3	$1 \rightarrow 3$	3	$9.9 \cdot 10^8$	$1.3 \cdot 10^{10}$	$7.1 \cdot 10^{10}$	$2.3 \cdot 10^{11}$	$5.6 \cdot 10^{11}$	$1.1 \cdot 10^{12}$	$2.0 \cdot 10^{12}$
VTS4	$1 \rightarrow 4$	1	$3.9 \cdot 10^{11}$	$1.2 \cdot 10^{12}$	$2.5 \cdot 10^{12}$	$4.3 \cdot 10^{12}$	$6.6 \cdot 10^{12}$	$8.8 \cdot 10^{12}$	$1.0 \cdot 10^{13}$
TS5	$1 \rightarrow 5$	1	$8.1 \cdot 10^6$	$6.8 \cdot 10^8$	$9.0 \cdot 10^9$	$5.1 \cdot 10^{10}$	$1.8 \cdot 10^{11}$	$4.9 \cdot 10^{11}$	$1.1 \cdot 10^{12}$
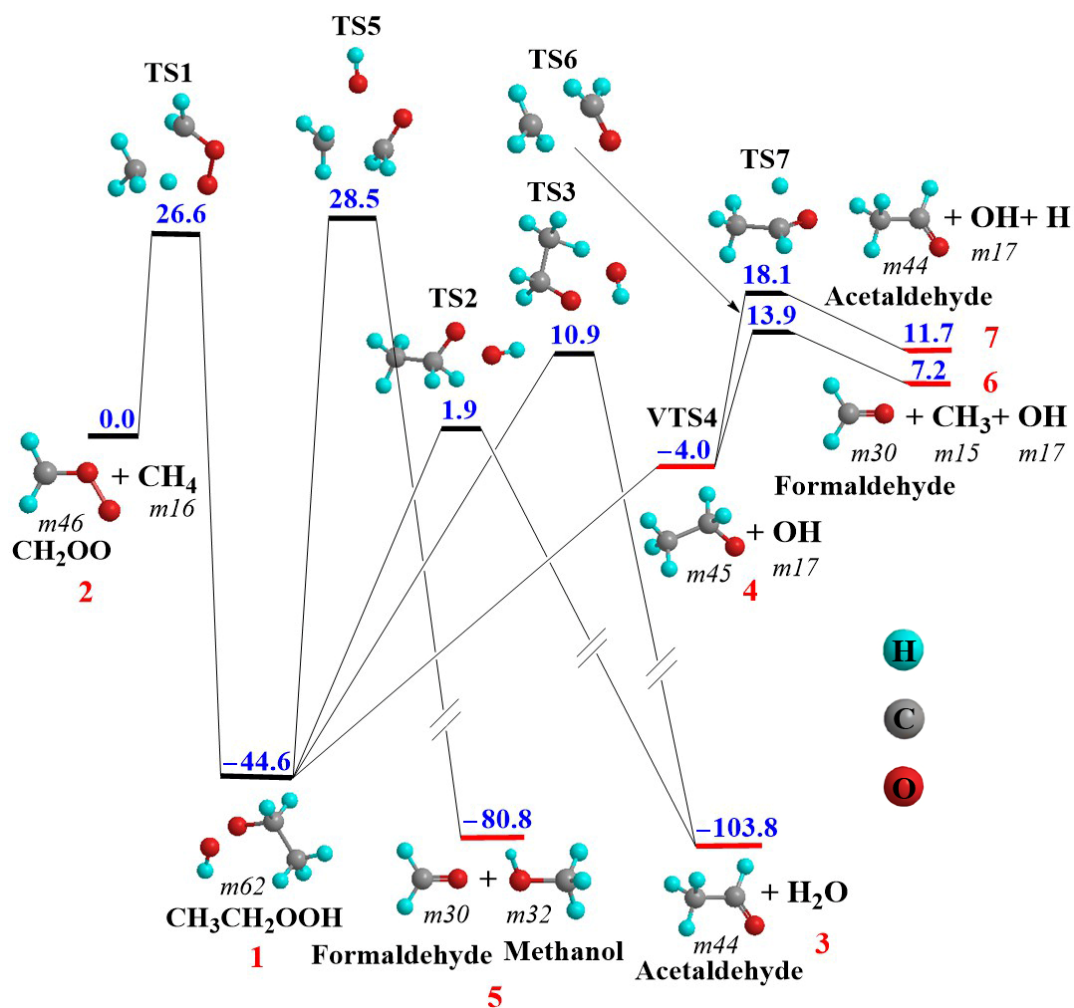
Figure 1. PESs of dissociation reactions initiated by collision of CH_2OO and methane. Blue numbers denote energies of transition states, intermediates, and reaction products (in kcal/mol). Red numbers denote numbering of isomers used in the table of rate constants and in figures of the reaction product yields. Italic numbers are the masses of molecules and fragments (in atomic units).

We can see that the lowest dissociation channel leads to the formation of two radicals, i.e., OH and CH_3CH_2O (designated as **4** in Figure 1; the virtual transition state of this reaction is designated as **VTS4**). This reaction occurs without a distinct transition state. In order to calculate the rate constant corresponding to this channel, we need to use the variational transition state approach [66], as described above and also in an earlier publication [67]. The rate constants related to the reactions presented in Figure 1 are calculated for different values of the vibrational internal energy of intermediate **1,** as given in Table 1. Note that in this work we have limited ourselves to the 100–250 kcal/mol energy range.

The relative product yields of the dissociation are shown in Figure 2. In this figure, the energy values are counted from isomer **1**. We see that the dominant dissociation channel over the entire energy range is channel **4** (formation of OH and CH_3CH_2O radicals). The two simultaneous reaction channels passing through barriers **TS2** and **TS3** lead to the same reaction product **3** (formation of acetaldehyde and H_2O) with substantial yield at high internal energy values. The third significant reaction path is the formation of formaldehyde and methanol (**5**), passing through the barrier **TS5**. But the branching ratio of this channel is relatively small and reaches a value of approximately 15% only on the right side of the plot. Channel **2**, which is the path providing the initial reagents $CH_2OO + CH_4$, is negligible, as

it was mentioned above. This means that for this collisional reaction, the reverse reaction leading to the formation of the initial reagents can be neglected.
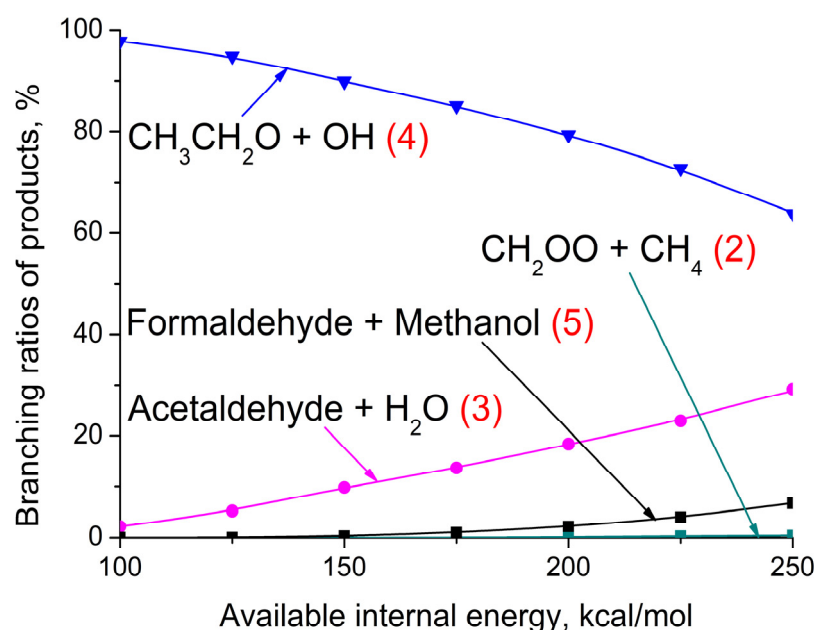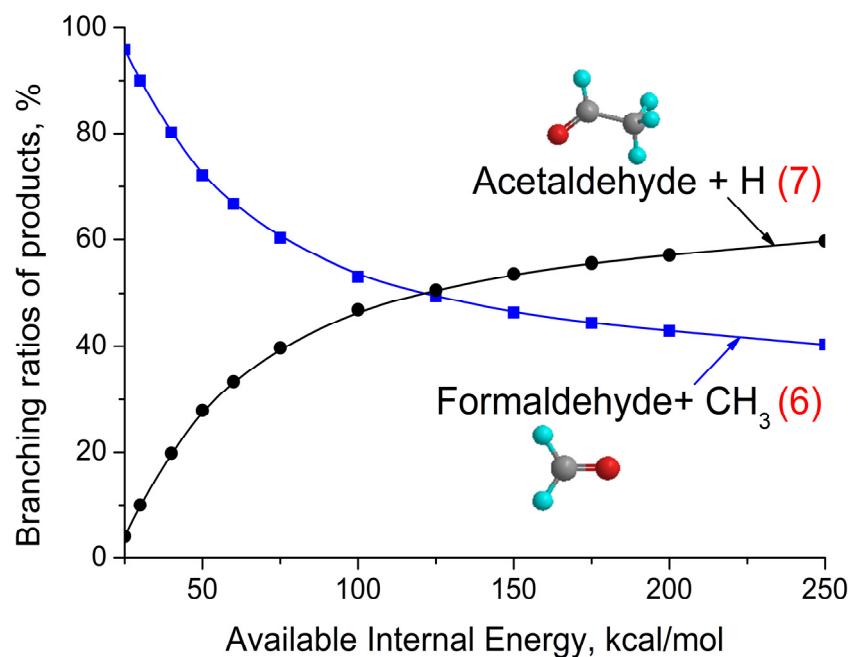

Figure 2. Relative product yields from the dissociation of isomer **1** (CH_3CH_2OOH) as a function of its internal energy. Red numbers in brackets denote the reaction channels indicated in Figure 1. The corresponding rate constants are given in Table 1.

It should be mentioned that according to Figure 1, products **3** and **5** have high energy release. Usually, it means that a significant amount of the released energy will be converted into the translational energy of products. So, these reactions could produce molecules with high translational energy, which may play an important role in the chemistry and physics of the upper atmosphere.

Considering the fact that in order to pass through barrier **TS1**, molecules have a kinetic energy no less than the barrier height (26.6 kcal/mol), and this energy will be transformed into the internal energy of the intermediate CH_3CH_2OOH. If there are no other sources of quick dissipation of the internal molecular energy at this altitude, it is sufficient for the OH group loss.

Products **4** (OH and CH_3CH_2O radicals) are formed without a distinct barrier. Numerous experiments with reactions in molecular beams show that during the barrierless cleavage of a single covalent bond, the fraction of energy converted into the kinetic energy of fragments is small and turns predominantly to vibrational energy. Therefore, we can assume that almost all the kinetic energy of the initial reagents, minus the value required to carry out the decomposition reaction through channel **VTS4**, will be converted into the internal energy of the products. It can be quite enough for secondary dissociation. In Figure 3, the secondary dissociation reaction of the CH_3CH_2O radical is shown. We do not know precisely which part of overall internal energy will be accumulated in this fragment, but for simplicity, we use the same 100–250 kcal/mol energy range. At low values of internal energy, the main dissociation products are formaldehyde and CH_3 radicals, with acetaldehyde and hydrogen atoms as minor products. The potential curves intersect at approximately 120 kcal/mol. According to these data, we conclude that formaldehyde and methyl radical will be the main products of the CH_2OO and CH_4 reactions at low energy collisions. At the same time, acetaldehyde, water, and hydrogen atoms will be the main reaction products at high energies.

Figure 3. Relative yield of reaction products formed as a result of the secondary dissociation of fragment CH_3CH_2O (reactions through **TS6** and **TS7** in Figure 1), which could occur due to the remaining internal energy. Red numbers in brackets denote the reaction channels indicated in Figure 1.

3.2. $CH_3CHOO + CH_4$ Reaction

The next collisional reaction that we shall discuss in this work is the reaction between methane and Criegee intermediate CH_3CHOO. This intermediate exists in two possible forms: *syn*-CH_3CHOO and *anti*-CH_3CHOO (see Figure 4), which differ in the spatial orientation of the COO group. The energy barrier of the rotation of this group around the C–O axis is about 34 kcal/mol, which is rather high and significantly exceeds the barrier for the OH group elimination reaction, i.e., 16.5 kcal/mol and 31.2 kcal/mol for *syn*- and *anti*-isomers, respectively. It is also higher than that of decomposition into other fragments. Their values range from 18.3 kcal/mol to 23.8 kcal/mol [30,31]. Therefore, these two isomers are considered, in general, to be different substances.

The *anti*-isomer reacts easily with water [15,16] and destroys it immediately near the earth's surface. Therefore, this isomer is not considered when describing processes occurring in the lower atmosphere. On the contrary, in rarefied upper atmospheric conditions, both isomers exist in comparable proportions [48] Supplementary Material.

The PES along possible routes of the collisional-induced chemical reactions between methane and CH_3CHOO are presented in Figure 4. As was mentioned above, in this work we do not discuss the direct formation of methanol due to collisions of the reagents. As in the previous part, we concentrate our attention on the formation of energetically stable single fragments, which then dissociate with the creation of various reaction products.

The entrance barrier for the collision-induced fusion reaction between methane and *anti*-CH_3CHOO (27.9 kcal/mol) or *syn*-CH_3CHOO (30.8 kcal/mol) is relatively high. However, as in the previous section, we believe that the total kinetic energy of reagents and the energy obtained during the synthesis of carbonyl oxide are sufficient to overcome the barrier. In the upper atmosphere, the energy obtained during the relaxation of excited states could also be added to this value.
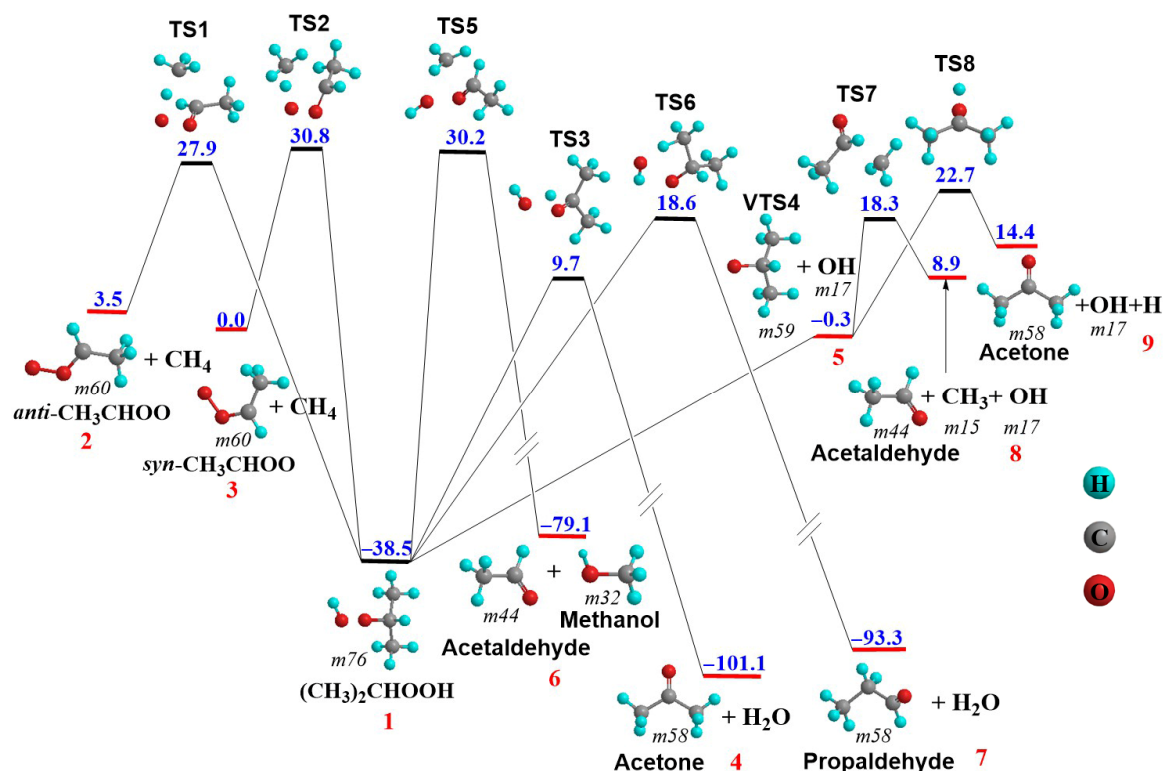
Figure 4. PESs of the dissociation reactions initiated by the collision of *syn*-CH$_3$CHOO and *anti*-CH$_3$CHOO with methane. Designations in this figure are the same as in Figure 1. Energies are measured in kcal/mol.

The result of this reaction is a large energy release (38.5 kcal/mol relative to the *syn*-CH$_3$CHOO + CH$_4$ level), which is finally transformed into the internal energy of the molecular complex (CH$_3$)$_2$CHOOH (denoted by **1**). For convenience, as in the previous section, we will consider this isomer as the starting point for all subsequent reactions.

As can be seen from Figure 4, the OH fragment is detached from the parent intermediate through **VTS4** without a distinct transition state, providing the formation of products **5**, i.e., OH and (CH$_3$)$_2$CHO radicals. Similar to the case discussed in the previous section, it implies that almost all the kinetic energy of the initial reagents, minus the value required to carry out the decomposition reaction through channel **VTS4**, will be transformed into the internal energy of the fragments. It can also be adequate for secondary dissociation.

The relative product yields of (CH$_3$)$_2$CHOOH isomer dissociation is shown in Figure 5. The rate constants used to prepare this figure are given in Table 2. One can see that the reaction with the formation of products **5** (OH and (CH$_3$)$_2$CHO radicals) dominates over the entire energy range. Reaction through **TS5** (with a barrier height of 30.5 kcal/mol), which provides the formation of acetaldehyde and methanol (product **6**), has a noticeable impact (up to 15% of the total amount of products) at high values of available internal energy. This reaction occurs through the shift of a weakly bonded OH fragment to one of the two available CH$_3$ groups. Therefore, the degeneracy of the reaction part is equal to 2. Usually, the barrier cross-section profile of this type of reaction is quite wide, which leads to an increase in the reaction rate constants.
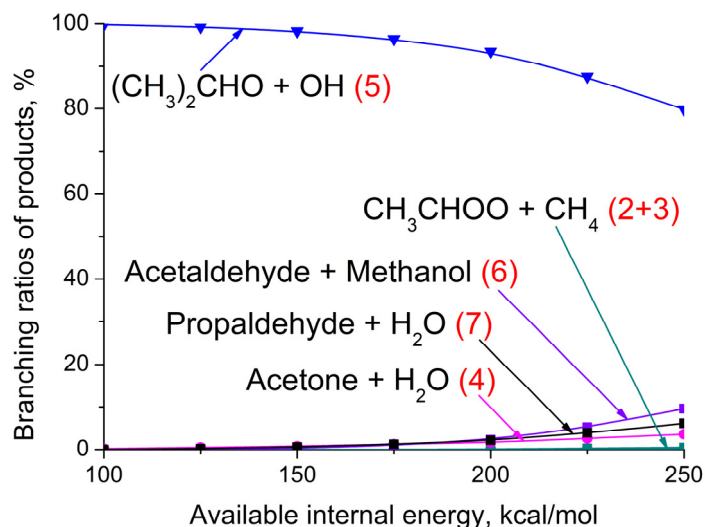
Figure 5. Relative product yields come from the dissociation of isomer **1** ((CH$_3$)$_2$CHOOH) as a function of its internal energy. Red numbers in brackets denote the reaction channels indicated in Figure 4. The corresponding rate constants are given in Table 2.

Table 2. RRKM and VTST unimolecular rate constants (s^{-1}) and reaction path degeneracies of dissociation initiated by collision of *syn*-CH$_3$CHOO and *anti*-CH$_3$CHOO CIs with methane. Energy values are measured from the energy of isomer 1 ((CH$_3$)$_2$CHOOH). Channels 2 and 3 are combined for simplicity.

| Transition State	Reaction	Reaction Path Degeneracy	Internal Energies, kcal/mol						
			100	125	150	175	200	225	250
TS1	$1 \rightarrow 2$	2	$3.6{\cdot}10^5$	$2.3{\cdot}10^7$	$3.2{\cdot}10^8$	$2.0{\cdot}10^9$	$7.6{\cdot}10^9$	$2.2{\cdot}10^{10}$	$5.6{\cdot}10^{10}$
TS2	$1 \rightarrow 3$	2	$7.0{\cdot}10^4$	$6.5{\cdot}10^6$	$1.1{\cdot}10^8$	$7.3{\cdot}10^8$	$3.0{\cdot}10^9$	$9.4{\cdot}10^9$	$2.3{\cdot}10^{10}$
TS3	$1 \rightarrow 4$	1	$2.1{\cdot}10^8$	$2.5{\cdot}10^9$	$1.3{\cdot}10^{10}$	$4.2{\cdot}10^{10}$	$1.0{\cdot}10^{11}$	$2.1{\cdot}10^{11}$	$3.8{\cdot}10^{11}$
VTS4	$1 \rightarrow 5$	1	$1.0{\cdot}10^{11}$	$5.2{\cdot}10^{11}$	$1.6{\cdot}10^{12}$	$3.3{\cdot}10^{12}$	$5.5{\cdot}10^{12}$	$6.9{\cdot}10^{12}$	$8.3{\cdot}10^{12}$
TS5	$1 \rightarrow 6$	2	$2.3{\cdot}10^6$	$2.6{\cdot}10^8$	$4.4{\cdot}10^9$	$3.2{\cdot}10^{10}$	$1.4{\cdot}10^{11}$	$4.2{\cdot}10^{11}$	$1.0{\cdot}10^{12}$
TS6	$1 \rightarrow 7$	6	$4.4{\cdot}10^7$	$1.1{\cdot}10^9$	$9.3{\cdot}10^9$	$4.2{\cdot}10^{10}$	$1.3{\cdot}10^{11}$	$3.2{\cdot}10^{11}$	$6.5{\cdot}10^{11}$

The path providing the formation of products **7** (propaldehyde and water) through the transition state **TS6** with a barrier of 18.6 kcal/mol is a minor channel. The reaction occurs through the shift of the OH fragment to one of the CH$_3$ groups, followed by the rearrangement of molecular geometry. The symmetry factor of this reaction is six because the parent molecule **1** has two CH$_3$ groups, and each of them has three equivalent hydrogen atoms. On the other hand, the C–H bond cleavage typically occurs through a barrier with a narrow cross-sectional profile, which usually decreases the rate constant and hence reduces the overall branching ratio.

The last reaction pathway (denoted as **4**) is the formation of acetone and water through **TS3** (with a barrier height of 9.7 kcal/mol). Despite its relatively low barrier height, the symmetry factor of this channel is equal to one, which reduces its contribution to the dissociation of initial isomer **1** and makes it a minor channel.

Thus, all the reactions except the pathway through **VTS4** have distinct barriers and are accompanied by significant energy releases. As noted above, a significant part of this energy can be transformed into the kinetic energy of products. Therefore, under certain conditions, these reactions could be a source of molecules with high kinetic energy. Backward reactions to the initial reagents (denoted as **2 + 3** in Figure 4) are negligible.

The results of branching ratio calculations performed for the secondary dissociation reaction of fragment (CH$_3$)$_2$CHO are presented in Figure 6. As in the previous section, our consideration here is performed in the same energy range of 100–250 kcal/mol. One

can see that the major reaction products, especially at low energy values, are acetaldehyde and methyl radical (denoted as **8**). The minor decomposition channel producing acetone and hydrogen atoms (denoted as **9** in Figure 6) has a significant branching ratio (up to 25%) only at high internal energy values. Therefore, this reaction can be a source of methyl radicals and hydrogen atoms, which are chemically active substances that can participate in many reactions, especially in the middle and upper atmosphere.
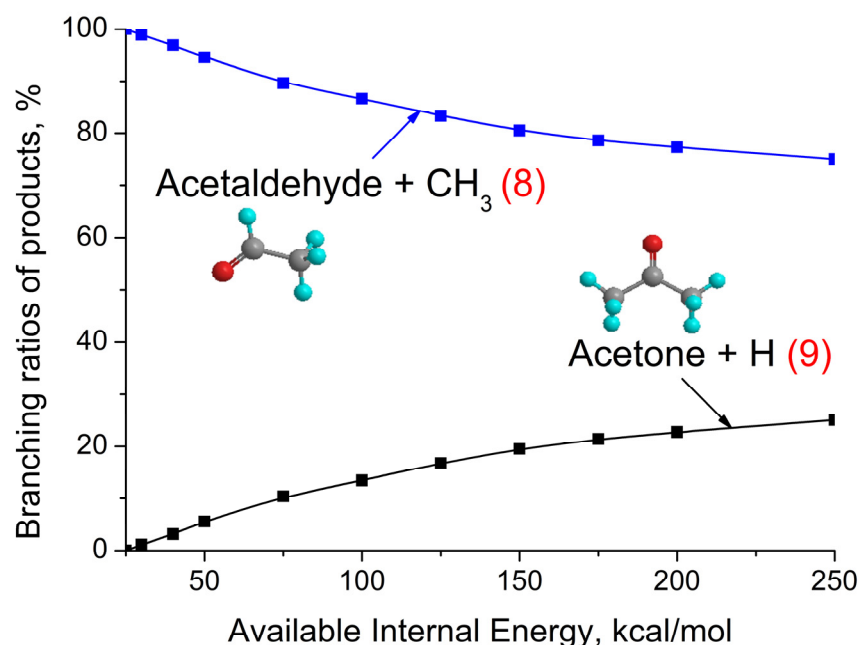
Figure 6. Relative yield of reaction products formed as a result of the secondary dissociation of fragment $(CH_3)_2CHO$ (reactions through **TS7** and **TS8** in Figure 4), which could occur due to the remaining internal energy. Red numbers in brackets denote the reaction channels indicated in Figure 4.

Based on the results presented in this section, it can also be noted that the heights of barriers, minima positions, and the final energy of the products have increased after replacing one hydrogen atom with a methyl group. Summarizing the results, we can conclude that chemical reactions caused by collisions between methane and Criegee intermediate CH_3CHOO can produce OH and CH_3 radicals, atomic hydrogen, methanol, acetaldehyde, water, and acetone. The exact product composition depends strongly on the initial internal and kinetic energy of the reagents.

3.3. $(CH_3)_2COO + CH_4$ Reaction

$(CH_3)_2COO$ molecules differ from the previously discussed CIs by the number of methyl groups. In this section, we will study the chemical reaction between this CI and methane. The overall potential energy surface of this reaction along the main pathways is presented in Figure 7. Similar to the case with CH_2OO and CH_3CHOO molecules, the reaction passes through the formation of a stable intermediate complex. In this case, the corresponding intermediate is $(CH_3)_3COOH$ (denoted as **1**). In order to achieve it, the reactants should overcome the entrance barrier **TS1** with a height of 31.2 kcal/mol. This value is higher than the corresponding ones for CH_2OO and CH_3CHOO molecules. The minimum depth of **1** (-34.7 kcal/mol) is also significantly higher than in the two previous cases. The energy of OH elimination channel **4** occurring through the variational transition state **VTS3** without a distinct barrier is 8.1 kcal/mol, which is also noticeably higher than in the previous two cases. We can conclude for these three reactions that the methylation effect is expressed in an increase in barrier heights, minima energies, and the quantity of

reaction products. It is also evident from the data presented in Tables 1–3 that the reaction rates decrease with an increase in the number of methyl groups.
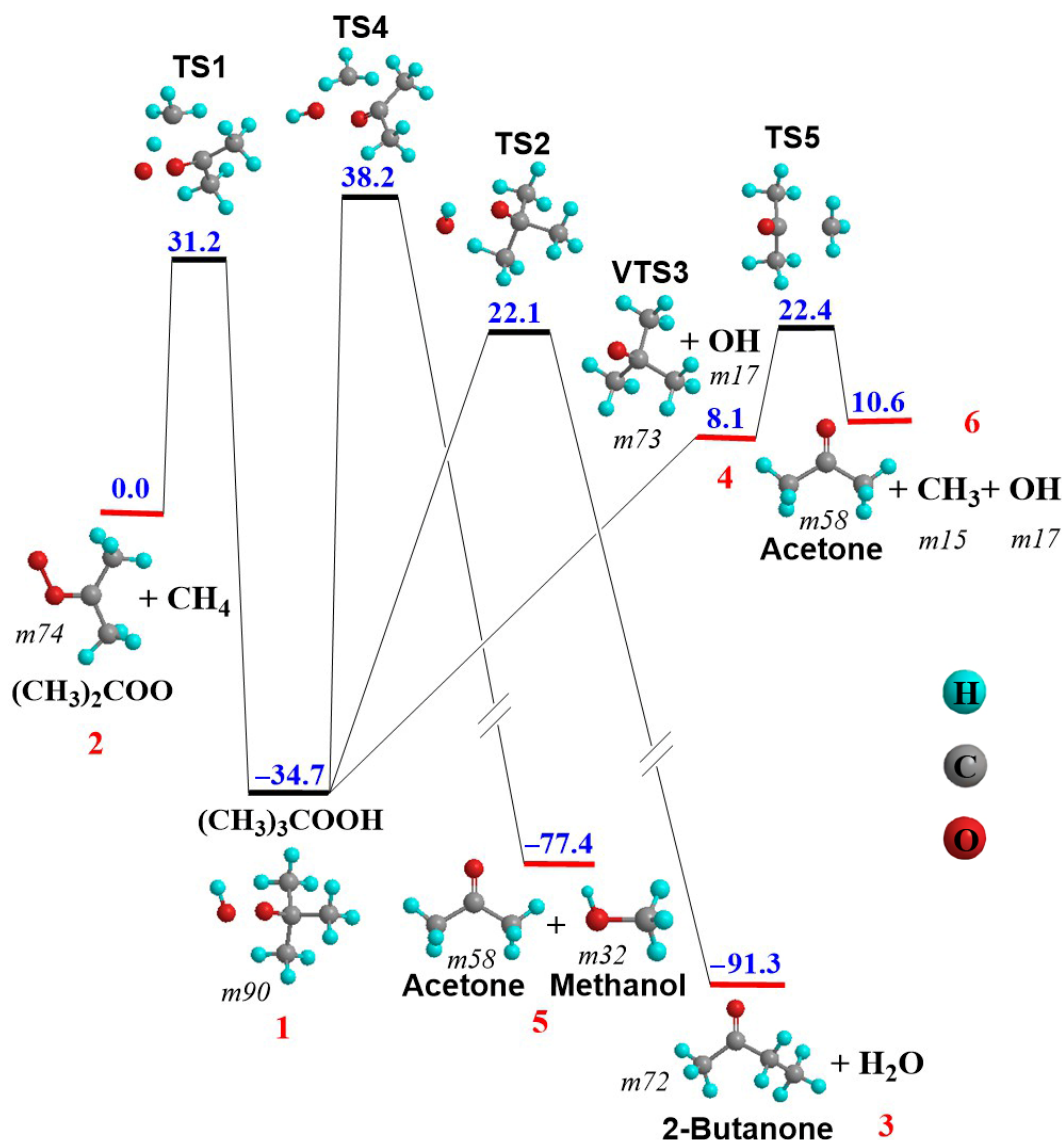
Figure 7. PESs of the dissociation reactions initiated by collision of $(CH_3)_2COO$ and methane. Designations in this figure are the same as in Figures 1 and 4. Energies are measured in kcal/mol.

**Table 3.** RRKM and VTST unimolecular rate constants (s^{-1}) and reaction path degeneracies of dissociation initiated by collision of $(CH_3)_3COO$ with methane. Energy values are measured from the energy of isomer 1 ($(CH_3)_3COOH$).

Transition State	Reaction	Reaction Path Degeneracy	Internal Energies, kcal/mol						
			100	125	150	175	200	225	250
TS1	$1 \rightarrow 2$	3	$3.0 \cdot 10^4$	$3.3 \cdot 10^6$	$6.2 \cdot 10^7$	$5.1 \cdot 10^8$	$2.4 \cdot 10^9$	$8.3 \cdot 10^9$	$2.2 \cdot 10^{10}$
TS2	$1 \rightarrow 3$	6	$2.7 \cdot 10^6$	$1.1 \cdot 10^8$	$1.2 \cdot 10^9$	$6.7 \cdot 10^9$	$2.4 \cdot 10^{10}$	$6.9 \cdot 10^{10}$	$2.6 \cdot 10^{11}$
VTS3	$1 \rightarrow 4$	1	$9.2 \cdot 10^9$	$6.1 \cdot 10^{10}$	$2.3 \cdot 10^{11}$	$5.3 \cdot 10^{11}$	$9.7 \cdot 10^{11}$	$1.6 \cdot 10^{12}$	$2.4 \cdot 10^{12}$
TS4	$1 \rightarrow 5$	3	$3.5 \cdot 10^3$	$1.5 \cdot 10^6$	$5.5 \cdot 10^7$	$6.5 \cdot 10^8$	$4.0 \cdot 10^9$	$1.7 \cdot 10^{10}$	$5.2 \cdot 10^{12}$

As in previous cases, we assume that almost the entire internal and kinetic energy of reactants transfers to the internal vibrational energy of intermediate **1**, i.e., it is at least higher than the depth of minimum **1** plus the height of the barrier **TS1**. It means that the internal

energy of the $(CH_3)_3COOH$ isomer is at least higher than 65.9 kcal/mol (31.2 + 34.7). The energy necessary to lose the OH group is equal to 42.8 kcal/mol (34.7 + 8.1). As it was mentioned above, the kinetic energy of fragments after dissociation without a barrier is small, so after the OH elimination, the complimentary fragment $(CH_3)_3CO$ could still have enough internal energy for a secondary reaction through barrier **TS5** (22.4 kcal/mol). The resulting products of this reaction will be acetone and methyl radicals.

The relative product yields of $(CH_3)_3COOH$ isomer dissociation are shown in Figure 8. The rate constants used to prepare this figure are given in Table 3. One can see that the major dissociation channel of isomer **1** in all energy ranges is the OH elimination reaction, which has been discussed already. The second possible reaction is the formation of 2-butanone (**3**) and water, which occurs through passing the barrier **TS2** (22.1 kcal/mol). The branching ratio of this reaction does not reach the value of 5% even at the highest values of internal energy. Reactions through **TS4** (38.2 kcal/mol), leading to the formation of acetone and methanol (**5**), as well as the backward reaction of the formation of initial reagents (**2**) via **TS1**, are negligible.
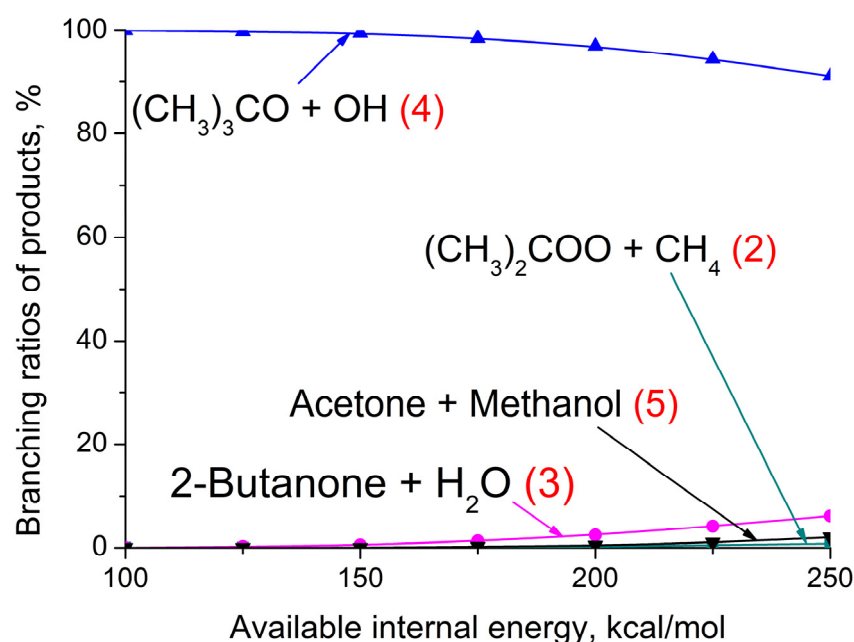
Figure 8. Relative product yields from dissociation of $(CH_3)_2COO$ as a function of its internal energy. Red numbers in brackets denote the reaction channels indicated in Figure 7. The corresponding rate constants are given in Table 3.

Summarizing the results for this section, we conclude that collision-induced chemical reactions between methane and $(CH_3)_2COO$ most probably produce acetone, OH, $(CH_3)_3CO$, and CH_3 radicals. Other fragments could be produced in insignificant amounts. The methylation effect is obviously presented in the case of this CI.

4. Conclusions

In this work, the chemical interaction between methane molecules and simple Criegee intermediates CH_2OO, *syn*-CH_3CHOO, *anti*-CH_3CHOO, and $(CH_3)_2COO$, initiated by collision, was studied. It has been shown that this interaction in the Earth's atmosphere, particularly in the upper atmosphere, leads to various chemical reactions, which result in the formation of many radicals such as OH, CH_3, ethoxy, methyletoxy, and others, as well as atomic hydrogen, methanol, acetone, water, and various aldehydes. CIs are extremely chemically active, and their presence in the atmosphere can initiate a large number of reactions. Methane is a major greenhouse gas that plays an important role in global warming. Our study has shown that both methane and CIs are destroyed during

their collision. This implies that this reaction should be considered as one of the ways to remove them from the atmosphere.

Many previous studies have shown that OH radicals are important "cleansers" of the atmosphere that remove air pollutants. They also participate in a large number of physical and chemical processes in the Earth's atmosphere, triggering cascades of cyclic secondary reactions, including the formation of atomic oxygen, HO_2, NO_2, hydrogen peroxide, etc. This work suggests a new possible source of hydroxyl radical formation.

The processes studied in this work also indicate probable new sources of atomic hydrogen, methanol, acetone, and water creation in the mesosphere and ionosphere. They may modify the chemical physics of these layers and initiate the creation of high-altitude stratospheric and noctilucent clouds. In addition, we have shown that methylation of this class of molecules increases reaction barriers and generally slows down the rates of chemical processes.

The high values of the entrance barriers of the collisional-induced reactions between methane and the simple CIs suggest that these reactions are most likely to occur in the rarefied layers of the upper atmosphere, where thermodynamic equilibrium is often disturbed and molecules with high kinetic energy are likely to be frequent. The processes leading to this conclusion are discussed above. There is also a high probability of the formation of electronically excited molecules in the upper atmosphere, for some of which the energy of electronic excitations then can be transformed into internal vibrational energy. Our calculations performed for a wide energy range of 100–250 kcal/mol should be useful for future studies of physicochemical processes in the upper atmosphere and ionosphere. Some questions concerning the probability and exact mechanisms of the formation of energetically cold and stable molecular complexes mentioned in this work require additional consideration. Photochemical processes occurring with the participation of electronically excited CIs and their molecular complexes are also very important. That is why the presented results may be useful in future studies of processes involving excited states of CIs.

References

1. Pachauri, R.K.; Meyer, L.A. (Eds.). *Climate Change 2014: Synthesis Report*; IPCC: Geneva, Switzerland, 2014; 151p.
2. Choi, W.; Kim, S.; Grant, W.B.; Shiotani, M.; Sasano, Y.; Schoeberl, M.R. Transport of methane in the stratosphere associated with the breakdown of the Antarctic polar vortex. *J. Geophys. Res. Atmos.* **2002**, *107*, D24. [CrossRef]
3. Nair, P.R.; Kavitha, M. Stratospheric distribution of methane over a tropical region as observed by MIPAS on board ENVISAT. *Int. J. Remote Sens.* **2020**, *41*, 8380–8405. [CrossRef]

4. Borchevkina, O.P.; Kurdyaeva, Y.A.; Dyakov, Y.A.; Karpov, I.V.; Golubkov, G.V.; Wang, P.K.; Golubkov, M.G. Disturbances of the thermosphere and the ionosphere during a meteorological storm. *Atmosphere* **2021**, *12*, 1384. [CrossRef]

5. Golubkov, G.V.; Adamson, S.O.; Borchevkina, O.P.; Wang, P.K.; Dyakov, Y.A.; Efishov, I.I.; Karpov, I.V.; Kurdyaeva, Y.A.; Lukhovitskaya, E.E.; Olkhov, O.A.; et al. Coupling of ionospheric disturbances with dynamic processes in the troposphere. *Russ. J. Phys. Chem. B* **2022**, *16*, 508–530. [CrossRef]

6. Mohammad, S.; Wang, P.K.; Chou, Y.L. A cloud model study of internal gravity wave breaking atop a high shear supercell in US high plains. *Russ. J. Phys. Chem. B* **2022**, *16*, 549–563. [CrossRef]

7. Shinbori, A.; Otsuka, Y.; Sori, T.; Nishioka, M.; Perwitasari, S.; Tsuda, T.; Nishitani, N. Electromagnetic conjugacy of ionospheric disturbances after the 2022 Hunga Tonga-Hunga Ha'apai volcanic eruption as seen in GNSS-TEC and SuperDARN Hokkaido pair of radars observations. *Earth Planets Sp.* **2022**, *74*, 106:1–106:17. [CrossRef]

8. Kesselmeier, J.; Staudt, M. Biogenic volatile organic compounds (VOC): An overview on emission, physiology and ecology. *J. Atmos. Chem.* **1999**, *33*, 23–88. [CrossRef]

9. Sindelarova, K.; Granier, C.; Bouarar, I.; Guenther, A.; Tilmes, S.; Stavrakou, T.; Müller, J.F.; Kuhn, U.; Stefani, P.; Knorr, W. Global data set of biogenic VOC emissions calculated by the MEGAN model over the last 30 years. *Atmos. Chem. Phys.* **2014**, *14*, 9317–9341. [CrossRef]

10. Levy, H. Normal atmosphere: Large radical and formaldehyde concentrations predicted. *Science* **1971**, *173*, 141–143. [CrossRef]

11. Lelieveld, J.; Dentener, F.J.; Peters, W.; Krol, M.C. On the role of hydroxyl radicals in the self-cleansing capacity of the troposphere. *Atmos. Chem. Phys.* **2004**, *4*, 2337–2344. [CrossRef]

12. Criegee, R.; Wenner, G. Die ozonisierung des 9,10-oktalins. *Justus Liebigs Ann. Chem.* **1949**, *564*, 9–15. [CrossRef]

13. Taatjes, C.A.; Welz, O.; Eskola, A.J.; Savee, J.D.; Scheer, A.M.; Shallcross, D.E.; Rotavera, B.; Lee, E.P.F.; Dyke, J.M.; Mok, D.K.W.; et al. Direct measurements of conformer-dependent reactivity of the Criegee intermediate CH_3CHOO. *Science* **2013**, *340*, 177–180. [CrossRef] [PubMed]

14. Wang, Y.Y.; Chung, C.Y.; Lee, Y.P. Infrared spectral identification of the Criegee intermediate $(CH3)_2COO$. *J. Chem. Phys.* **2016**, *145*, 154303:1–154303:6. [CrossRef]

15. Chao, W.; Hsieh, J.T.; Chang, C.H.; Lin, J.J.M. Direct kinetic measurement of the reaction of the simplest Criegee intermediate with water vapor. *Science* **2015**, *347*, 751–754. [CrossRef] [PubMed]

16. Long, B.; Bao, J.L.; Truhlar, D.G. Atmospheric chemistry of Criegee intermediates: Unimolecular reactions and reactions with water. *J. Am. Chem. Soc.* **2016**, *138*, 14409–14422. [CrossRef]

17. Smith, M.C.; Chang, C.H.; Chao, W.; Lin, L.C.; Takahashi, K.; Boering, K.A.; Lin, J.J.M. Strong negative temperature dependence of the simplest Criegee intermediate CH_2OO reaction with water dimer. *J. Phys. Chem. Lett.* **2015**, *6*, 2708–2713. [CrossRef]

18. Lin, L.C.; Chang, H.T.; Chang, C.H.; Chao, W.; Smith, M.C.; Chang, C.H.; Lin, J.J.M.; Takahashi, K. Competition between H_2O and $(H_2O)_2$ reactions with CH_2OO/CH_3CHOO. *Phys. Chem. Chem. Phys.* **2016**, *18*, 4557–4568. [CrossRef]

19. Sheps, L.; Scully, A.M.; Au, K. UV absorption probing of the conformer-dependent reactivity of a Criegee intermediate CH_3CHOO. *Phys. Chem. Chem. Phys.* **2014**, *16*, 26701–26706. [CrossRef]

20. Welz, O.; Eskola, A.J.; Sheps, L.; Rotavera, B.; Savee, J.D.; Scheer, A.M.; Osborn, D.L.; Lowe, D.; Murray Booth, A.; Xiao, P.; et al. Rate coefficients of C1 and C2 Criegee intermediate reactions with formic and acetic acid near the collision limit: Direct kinetics measurements and atmospheric implications. *Angew. Chemie Int. Ed.* **2014**, *53*, 4547–4550. [CrossRef]

21. Taatjes, C.A.; Shallcross, D.E.; Percival, C.J. Research frontiers in the chemistry of Criegee intermediates and tropospheric ozonolysis. *Phys. Chem. Chem. Phys.* **2014**, *16*, 1704–1718. [CrossRef]

22. Foreman, E.S.; Kapnas, K.M.; Murray, C. Reactions between Criegee intermediates and the inorganic acids HCl and HNO_3: Kinetics and atmospheric implications. *Angew. Chemie Int. Ed.* **2016**, *55*, 10419–10422. [CrossRef]

23. Chhantyal-Pun, R.; McGillen, M.R.; Beames, J.M.; Khan, M.A.H.; Percival, C.J.; Shallcross, D.E.; Orr-Ewing, A.J. Temperature-dependence of the rates of reaction of trifluoroacetic acid with Criegee intermediates. *Angew. Chemie Int. Ed.* **2017**, *56*, 9044–9047. [CrossRef] [PubMed]

24. Khan, M.A.H.; Percival, C.J.; Caravan, R.L.; Taatjes, C.A.; Shallcross, D.E. Criegee intermediates and their impacts on the troposphere. *Environ. Sci. Process. Impacts* **2018**, *20*, 437–453. [CrossRef] [PubMed]

25. Behera, B.; Takahashi, K.; Lee, Y.P. Mechanism and kinetics of the reaction of the Criegee intermediate CH_2OO with acetic acid studied using a step-scan Fourier-transform IR spectrometer. *Phys. Chem. Chem. Phys.* **2022**, *24*, 18568–18581. [CrossRef] [PubMed]

26. Kanakidou, M.; Seinfeld, J.H.; Pandis, S.N.; Barnes, I.; Dentener, F.J.; Facchini, M.C.; Van Dingenen, R.; Ervens, B.; Nenes, A.; Nielsen, C.J.; et al. Organic aerosol and global climate modelling: A review. *Atmos. Chem. Phys.* **2005**, *5*, 1053–1123. [CrossRef]

27. Hallquist, M.; Wenger, J.C.; Baltensperger, U.; Rudich, Y.; Simpson, D.; Claeys, M.; Dommen, J.; Donahue, N.M.; George, C.; Goldstein, A.H.; et al. The formation, properties and impact of secondary organic aerosol: Current and emerging issues. *Atmos. Chem. Phys.* **2009**, *9*, 5155–5236. [CrossRef]

28. Taatjes, C.A.; Khan, M.A.H.; Eskola, A.J.; Percival, C.J.; Osborn, D.L.; Wallington, T.J.; Shallcross, D.E. Reaction of perfluorooctanoic acid with Criegee intermediates and implications for the atmospheric fate of perfluorocarboxylic acids. *Environ. Sci. Technol.* **2019**, *53*, 1245–1251. [CrossRef] [PubMed]

29. Herron, J.T.; Martinez, R.I.; Huie, R.E. Kinetics and energetics of the Criegee intermediate in the gas phase. II. The Criegee intermediate in the photooxidation of formaldehyde, in alkyldioxy disproportionation and O + oxoalkane addition reactions. *Int. J. Chem. Kinet.* **1982**, *14*, 225–236. [CrossRef]

30. Wang, Z.; Dyakov, Y.A.; Bu, Y. Dynamics insight into isomerization and dissociation of hot Criegee intermediate CH₃CHOO. *J. Phys. Chem. A* **2019**, *123*, 1085–1090. [CrossRef]

31. Dyakov, Y.A.; Adamson, S.O.; Wang, P.K.; Golubkov, G.V.; Olkhov, O.A.; Peskov, V.D.; Rodionov, I.D.; Rodionova, I.P.; Rodionov, A.I.; Shapovalov, V.L.; et al. Isomerization and decay of a Criegee intermediate CH₃CHOO in the Earth's upper atmosphere. *Russ. J. Phys. Chem. B* **2021**, *15*, 559–565. [CrossRef]

32. Stone, D.; Au, K.; Sime, S.; Medeiros, D.J.; Blitz, M.; Seakins, P.W.; Decker, Z.; Sheps, L. Unimolecular decomposition kinetics of the stabilised Criegee intermediates CH₂OO and CD₂OO. *Phys. Chem. Chem. Phys.* **2018**, *20*, 24940–24954. [CrossRef]

33. Fang, Y.; Liu, F.; Barber, V.P.; Klippenstein, S.J.; McCoy, A.B.; Lester, M.I. Communication: Real time observation of unimolecular decay of Criegee intermediates to OH radical products. *J. Chem. Phys.* **2016**, *144*, 061102:1–061102:4. [CrossRef]

34. Kidwell, N.M.; Li, H.; Wang, X.; Bowman, J.M.; Lester, M.I. Unimolecular dissociation dynamics of vibrationally activated CH₃CHOO Criegee intermediates to OH radical products. *Nat. Chem.* **2016**, *8*, 509–514. [CrossRef] [PubMed]

35. Wang, X.; Bowman, J.M. Two pathways for dissociation of highly energized syn-CH₃CHOO to OH plus vinoxy. *J. Phys. Chem. Lett.* **2016**, *7*, 3359–3364. [CrossRef] [PubMed]

36. Nguyen, T.L.; McCaslin, L.; McCarthy, M.C.; Stanton, J.F. Communication: Thermal unimolecular decomposition of syn-CH₃CHOO: A kinetic study. *J. Chem. Phys.* **2016**, *145*, 131102:1–131102:5. [CrossRef] [PubMed]

37. Zhou, X.; Liu, Y.; Dong, W.; Yang, X. Unimolecular reaction rate measurement of syn-CH₃CHOO. *J. Phys. Chem. Lett.* **2019**, *10*, 4817–4821. [CrossRef]

38. Beames, J.M.; Liu, F.; Lu, L.; Lester, M.I. UV spectroscopic characterization of an alkyl substituted Criegee intermediate CH₃CHOO. *J. Chem. Phys.* **2013**, *138*, 244307:1–244307:9. [CrossRef]

39. Sheps, L. Absolute ultraviolet absorption spectrum of a Criegee intermediate CH₂OO. *J. Phys. Chem. Lett.* **2013**, *4*, 4201–4205. [CrossRef]

40. Liu, F.; Beames, J.M.; Green, A.M.; Lester, M.I. UV spectroscopic characterization of dimethyl- and ethyl-substituted carbonyl oxides. *J. Phys. Chem. A* **2014**, *118*, 2298–2306. [CrossRef]

41. Ting, W.L.; Chen, Y.H.; Chao, W.; Smith, M.C.; Lin, J.J.M. The UV absorption spectrum of the simplest Criegee intermediate CH₂OO. *Phys. Chem. Chem. Phys.* **2014**, *16*, 10438–10443. [CrossRef]

42. Samanta, K.; Beames, J.M.; Lester, M.I.; Subotnik, J.E. Quantum dynamical investigation of the simplest Criegee intermediate CH₂OO and its O–O photodissociation channels. *J. Chem. Phys.* **2014**, *141*, 134303:1–134303:12. [CrossRef] [PubMed]

43. Lee, Y.P. Perspective: Spectroscopy and kinetics of small gaseous Criegee intermediates. *J. Chem. Phys.* **2015**, *143*, 020901:1–020901:16. [CrossRef] [PubMed]

44. Ting, A.W.L.; Lin, J.J.M. UV Spectrum of the simplest deuterated Criegee intermediate CD₂OO. *J. Chinese Chem. Soc.* **2017**, *64*, 360–368. [CrossRef]

45. Esposito, V.J.; Werba, O.; Bush, S.A.; Marchetti, B.; Karsili, T.N.V. Insights into the ultrafast dynamics of CH₂OO and CH₃CHOO following excitation to the bright 1 ππ* state: The role of singlet and triplet states. *Photochem. Photobiol.* **2022**, *98*, 763–772. [CrossRef] [PubMed]

46. Lin, M.F.; Tzeng, C.M.; Dyakov, Y.A.; Ni, C.K. Photostability of amino acids: Internal conversion versus dissociation. *J. Chem. Phys.* **2007**, *126*, 241104:1–241104:5. [CrossRef] [PubMed]

47. Dyakov, Y.A.; Toliautas, S.; Trakhtenberg, L.I.; Valkunas, L. Excited state photodissociation dynamics of 2-, 3-, 4-hydroxyacetophenone: Theoretical study. *Chem. Phys.* **2018**, *515*, 672–678. [CrossRef]

48. Dyakov, Y.A.; Adamson, S.O.; Wang, P.K.; Vetchinkin, A.S.; Golubkov, G.V.; Peskov, V.D.; Rodionov, I.D.; Syromyatnikov, A.G.; Umanskii, S.Y.; Shestakov, D.V.; et al. Excited state dynamics of CH₃CHOO Criegee intermediates in the upper atmosphere of the Earth. *Russ. J. Phys. Chem. B* **2022**, *16*, 543–548. [CrossRef]

49. Larsson, M.; Orel, A.E. *Dissociative Recombination of Molecular Ions*; Cambridge University Press: Cambridge, UK, 2008; 392p.

50. Hsu, C.H.; Tsai, M.T.; Dyakov, Y.A.; Ni, C.K. Energy transfer of highly vibrationally excited molecules studied by crossed molecular beam/time-sliced velocity map ion imaging. *Int. Rev. Phys. Chem.* **2012**, *31*, 201–233. [CrossRef]

51. Huang, H.L.; Chao, W.; Lin, J.J.M. Kinetics of a Criegee intermediate that would survive high humidity and may oxidize atmospheric SO₂. *Proc. Natl. Acad. Sci. USA* **2015**, *112*, 10857–10862. [CrossRef]

52. Mauldin III, R.L.; Berndt, T.; Sipilä, M.; Paasonen, P.; Petäjä, T.; Kim, S.; Kurtén, T.; Stratmann, F.; Kerminen, V.M.; Kulmala, M. A new atmospherically relevant oxidant of sulphur dioxide. *Nature* **2012**, *488*, 193–196. [CrossRef]

53. Kumar, M.; Francisco, J.S. Reactions of Criegee intermediates with non-water greenhouse gases: Implications for metal free chemical fixation of carbon dioxide. *J. Phys. Chem. Lett.* **2017**, *8*, 4206–4213. [CrossRef] [PubMed]

54. Xu, K.; Wang, W.; Wei, W.; Feng, W.; Sun, Q.; Li, P. Insights into the reaction mechanism of Criegee intermediate CH₂OO with methane and implications for the formation of methanol. *J. Phys. Chem. A* **2017**, *121*, 7236–7245. [CrossRef] [PubMed]

55. Dyakov, Y.A.; Adamson, S.O.; Wang, P.K.; Vetchinkin, A.S.; Golubkov, G.V.; Morozov, I.I.; Umanskii, S.Y.; Chaikina, Y.A.; Golubkov, M.G. Collisional dissociation of Crieege CH₃CHOO and methane intermediates in the Earth's upper atmosphere. *Russ. J. Phys. Chem. B* **2021**, *15*, 782–788. [CrossRef]

56. Kalinowski, J.; Foreman, E.S.; Kapnas, K.M.; Murray, C.; Räsänen, M.; Benny Gerber, R. Dynamics and spectroscopy of CH_2OO excited electronic states. *Phys. Chem. Chem. Phys.* **2016**, *18*, 10941–10946. [CrossRef] [PubMed]

57. Li, Y.; Gong, Q.; Yue, L.; Wang, W.; Liu, F. Photochemistry of the simplest Criegee intermediate, CH_2OO: Photoisomerization channel toward dioxirane revealed by CASPT2 calculations and trajectory surface-hopping dynamics. *J. Phys. Chem. Lett.* **2018**, *9*, 978–981. [CrossRef]

58. Marchetti, B.; Esposito, V.J.; Bush, R.E.; Karsili, T.N.V. The states that hide in the shadows: The potential role of conical intersections in the ground state unimolecular decay of a Criegee intermediate. *Phys. Chem. Chem. Phys.* **2022**, *24*, 532–540. [CrossRef] [PubMed]

59. Becke, A.D. Density-functional thermochemistry. I. The effect of the exchange-only gradient correction. *J. Chem. Phys.* **1992**, *96*, 2155–2160. [CrossRef]

60. Becke, A.D. Density-functional thermochemistry. II. The effect of the Perdew–Wang generalized-gradient correlation correction. *J. Chem. Phys.* **1992**, *97*, 9173–9177. [CrossRef]

61. Becke, A.D. Density-functional thermochemistry. III. The role of exact exchange. *J. Chem. Phys.* **1993**, *98*, 5648–5652. [CrossRef]

62. Lee, C.; Yang, W.; Parr, R.G. Development of the Colle-Salvetti correlation-energy formula into a functional of the electron density. *Phys. Rev. B* **1988**, *37*, 785–789. [CrossRef]

63. Frisch, M.J.; Trucks, G.W.; Schlegel, H.B.; Scuseria, G.E.; Robb, M.A.; Cheeseman, J.R.; Scalmani, G.; Barone, V.; Petersson, G.A.; Nakatsuji, H.; et al. *Gaussian 09, Revision A.02*; Gaussian, Inc.: Wallingford, CT, USA, 2009.

64. Eyring, H.; Lin, S.H.; Lin, S.M. *Basic Chemical Kinetics*; JohnWiley & Sons: New York, NY, USA, 1980; 493p.

65. Robinson, P.J.; Holbrook, K.A. *Unimolecular Reactions*; JohnWiley & Sons: New York, NY, USA, 1972; 372p.

66. Steinfeld, J.I.; Francisco, J.S.; Hase, W.L. *Chemical Kinetics and Dynamics*; Prentice Hall: Upper Saddle River, NJ, USA, 1999; 518p.

67. Kislov, V.V.; Nguyen, T.L.; Mebel, A.M.; Lin, S.H.; Smith, S.C. Photodissociation of benzene under collision-free conditions: An ab initio/Rice–Ramsperger–Kassel–Marcus study. *J. Chem. Phys.* **2004**, *120*, 7008–7017. [CrossRef] [PubMed]